JACS
JOURNAL OF THE AMERICAN CHEMICAL SOCIETY

COMMUNICATION

pubs.acs.org/JACS

Adiabatic Versus Nonadiabatic Photoisomerization in Photochromic Ruthenium Sulfoxide Complexes: A Mechanistic Picture from Density Functional Theory Calculations.

Adrien J. Göttle, Isabelle M. Dixon, Fabienne Alary, Jean-Louis Heully, and Martial Boggio-Pasqua*

Laboratoire de Chimie et Physique Quantiques - IRSAMC, CNRS et Université de Toulouse, 31062 Toulouse, France

Supporting Information

ABSTRACT: Polypyridine ruthenium sulfoxide complexes are intriguing compounds which can display both photochromic and electrochromic properties. These properties are based on the Ru−S → Ru−O linkage isomerization capability of the sulfoxide group. The photoisomerization mechanism is of particular importance in order to understand the photophysical properties of such molecules. Density functional theory calculations demonstrate that the main photoisomerization mechanism is nonadiabatic for the system under study in agreement with the experimental observations. Indeed, funnels for efficient radiationless decay back to the ground state are shown to be easily accessible compared to transition states on the adiabatic triplet potential energy surface. However, we highlight for the first time that triplet metal-centered states play a central role in the photoisomerization mechanism of these compounds.

Isomerization in photochromic polypyridine ruthenium sulfoxide complexes has attracted considerable interest over the past decade. The group of J. J. Rack have developed this class of photochromic and electrochromic compounds, which can undergo intramolecular isomerization of the sulfoxide from *S*-bonded to *O*-bonded, triggered either by light or by formal oxidation.[1−17] Their most exciting experimental observations were recently summarized in a short review article.[18] On the other hand, very few theoretical studies have been devoted to these systems. The most noteworthy contribution comes from the work of Ciofini et al.,[19] in which the photoisomerization mechanism of a ruthenium dimethyl sulfoxide complex $[Ru(bpy)(tpy)(dmso)]^{2+}$ (bpy = 2,2′-bipyridine; tpy = 2,2′:6′,2″-terpyridine; dmso = dimethyl sulfoxide) was investigated by means of density functional theory. This theoretical work shed some light on the spectroscopic properties of the complex. In particular, it showed that the η^2 *SO*-linked form, found along the Ru−S → Ru−O linkage isomerization coordinate, was not responsible for the luminescence properties of the complex. Rather, this structure was described as a transition state and the change in the emission spectra observed after photoexcitation was assigned to the *S*-bonded and *O*-bonded triplet metal-to-ligand charge transfer (MLCT) states.

Photoisomerization of the $[Ru(bpy)(tpy)(dmso)]^{2+}$ complex and other monodentate sulfoxide ruthenium complexes were shown to be mainly adiabatic on the lowest triplet MLCT state by transient absorption spectroscopy.[18] However, McClure et al. recently synthesized chelating sulfoxide complexes such as $[Ru(bpy)_2(OSO)]^+$ (OSO = 2-methylsulfinylbenzoate, see Figure 1) for which nonadiabatic photoisomerization was deduced from the absence of spectroscopic and kinetic signatures of an *O*-bonded ^{3}MLCT state.[15] The photoisomerization was suspected to occur nonadiabatically from an *S*-bonded ^{3}MLCT state or from an η^2-sulfoxide species. In this study, we report a detailed computational study of the complete triplet excited-state isomerization pathway of the $[Ru(bpy)_2(OSO)]^+$ complex, considering both adiabatic and nonadiabatic routes. The results are summarized in Figure 2. We show indeed that nonadiabatic photoisomerization will be favored over adiabatic photoisomerization. However, we also demonstrate that, unlike what was proposed so far, if the photoisomerization takes place on the lowest triplet potential energy surface (PES), triplet metal-centered (MC) states (also called ligand-field states) will be involved in both the adiabatic and nonadiabatic processes.

Figure 2 summarizes the complete potential energy profile on the lowest adiabatic triplet excited state along the *S*-bonded to *O*-bonded photoisomerization pathway. This profile was deduced from density functional theory calculations (computational details in Supporting Information [SI]). Table 1 collects all the relative energies between the various minima and transition states involved in this multistep process. Details of all the molecular and electronic structures are given in the SI (Tables S1−S11). It is known experimentally that initial photoexcitation produces a ^{1}MLCT state, which relaxes to a thermally equilibrated ^{3}MLCT state within a few picoseconds. Two structures, denoted *S*-MLCT$_1$ and *S*-MLCT$_2$, corresponding to the same electronic ^{3}MLCT state, were identified as the initial thermally equilibrated ^{3}MLCT state. They interchange via torsion of the carboxylate group (Figure S1 and animation 1 in SI), the $O_3-C_1-C_2-C_3$ dihedral angle varying from 36.9° to 11.3° to −16.1° at the *S*-MLCT$_1$, *S*-MLCT-TS, and *S*-MLCT$_2$, respectively (Tables S1−S3, SI). The activation barrier associated with this torsion was computed at ∼5 kJ/mol in methanol, consistent with an equilibrated ^{3}MLCT state between the two isomers.

From the *S*-MLCT$_2$ species, the system can relax to a triplet MC state denoted *S*-MC$_1$ via the transition state *S*-MLCT-MC-TS. This step mainly corresponds to an elongation of the Ru−S bond from 2.340 Å to 2.746 Å (Figure S2 and animation 2 in SI). At the transition state, the Ru−S distance is 2.550 Å, and the

Received: February 21, 2011
Published: May 23, 2011

dx.doi.org/10.1021/ja201625b | *J. Am. Chem. Soc.* 2011, 133, 9172–9174

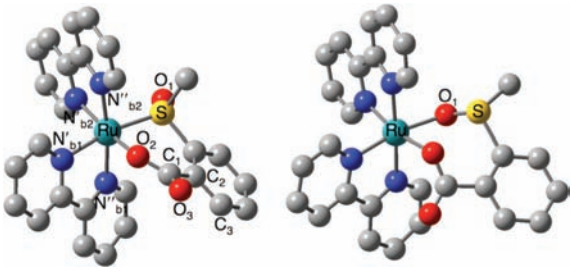

Figure 1. Schematic representation and labeling scheme for the *S*-bonded (left) and *O*-bonded (right) isomers of $[Ru(bpy)_2(OSO)]^+$.

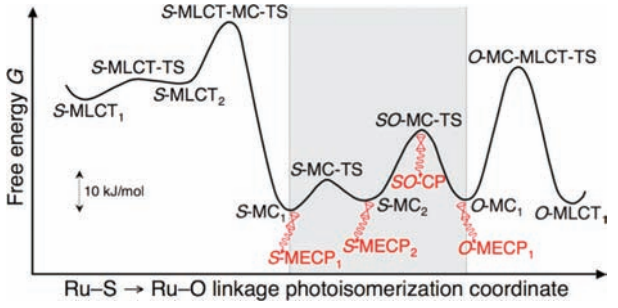

Figure 2. Schematic representation of the lowest triplet excited-state free energy profile in methanol. The adiabatic pathway is shown as the black line, the region where nonadiabatic transitions can occur is shaded, and funnels for such transitions are shown in red. The profile was deduced from all the data given in Supporting Information.

activation barrier is only 13.5 kJ/mol. The minimum *S*-MC_1 lies 30.7 kJ/mol below the *S*-$MLCT_2$ species and is expected to be populated as it is thermodynamically more stable. In addition to the Ru−S bond stretching that occurs, it is worthwhile noting that the angle between the two bipyridine ligands opens up. Indeed, the N'_{b1}−Ru−N'_{b2} angle changes from 96.0° at *S*-$MLCT_2$, to 112.6° at *S*-MLCT-MC-TS, to 132.8° at *S*-MC_1 (Tables S3−S5, SI). In the end, at the *S*-MC_1 minimum, the complex is almost pentacoordinated.

In the next step from *S*-MC_1 to *S*-MC_2 via the *S*-MC-TS transition state, the Ru−S and Ru−N'_{b1} bonds get further elongated by ∼0.2 Å, and the angle between the two bipyridine ligands closes up again to 96.8° (Figure S3 and animation 3 in SI). Thus, the arrangement of the two bipyridine ligands better resembles that in the octahedral environment with two ligands, the sulfoxide and the bipyridine nitrogen in the trans position, partially de-coordinated. The two species *S*-MC_1 and *S*-MC_2 are almost isoenergetic, and the activation barrier involved is about 7 kJ/mol (Tables S5−S7, SI).

The fourth step is the critical step for *S*-linked to *O*-linked adiabatic isomerization (Tables S7−S9, SI). The main coordinate involves a rotation of the sulfoxide group (Figure S4 and animation 4 in SI). The transition state *SO*-MC-TS corresponds to an asymmetric η^2 *SO*-linked structure with Ru−S and Ru−O_1 distances of 3.158 Å and 3.468 Å, respectively. The activation barrier for this isomerization is computed at 16.1 kJ/mol. The resulting species is an *O*-linked MC state, denoted *O*-MC_1, in which the Ru−O_1 bond length is reduced to 2.559 Å. This species is of similar energy as the *S*-linked MC state.

Finally, the last adiabatic step along the photoisomerization pathway involves the formation of the new Ru−O_1 bond via

Table 1. Energies and Gibbs Energies at 298 K (in kJ/mol) along the Adiabatic *S*-Bonded to *O*-Bonded Photoisomerization on the Lowest Triplet Potential Energy Surface

structures	ΔE^a	ΔG^b	ΔG_s^c
S-$MLCT_1$	0.0	0.0	0.0
S-MLCT-TS	12.3	10.2	4.6
S-$MLCT_2$	4.4	3.7	4.9
S-MLCT-MC-TS	26.7	21.4	18.4
S-MC_1	−3.5	−10.7	−25.8
S-MC-TS	−3.4	−7.5	−18.7
S-MC_2	−7.1	−14.8	−23.1
SO-MC-TS	6.6	0.4	−7.0
O-MC_1	−24.6	−33.2	−23.2
O-MC-MLCT-TS	2.5	−5.1	7.8
O-$MLCT_1$	−34.8	−33.8	−24.1

[a] Gas phase energies relative to *S*-$MLCT_1$. [b] Gas phase Gibbs energies relative to *S*-$MLCT_1$. [c] Gibbs energies in methanol relative to *S*-$MLCT_1$.

population of an *O*-bonded MLCT state, *O*-$MLCT_1$, which is isoenergetic with *O*-MC_1 (Tables S9−S11, SI). The main coordinate involves the re-coordination of N'_{b1} (Ru−N'_{b1} = 2.024 Å) and the formation of the new Ru−O_1 bond (Ru−O_1 = 2.066 Å) (Figure S5 and animation 5 in SI). This step involves by far the largest activation energy at 31 kJ/mol, and thus is the rate-limiting step in the adiabatic photoisomerization.

The five-step process described above represents the complete adiabatic photoisomerization pathway that takes place on the lowest triplet potential energy surface. However, the experimental evidence points to a nonadiabatic photoisomerization, where an η^2-sulfoxide bonding structure was suspected to be the main candidate for the photochemical funnel responsible for the nonadiabatic transitions back to the ground state.[15,18] Therefore, we investigated nonadiabatic pathways by searching critical structures called crossing points (CP) where the lowest triplet state is degenerate with the ground state (in SI see computational details and Figure S6). Figure 2 reveals four of these structures for which radiationless decay to the ground state could be efficient. First, at the *SO*-MC-TS transition state structure, we found that the triplet/singlet energy gap is only 6.1 kJ/mol. Thus, it confirms the experimental assumption of a possible η^2-type funnel,[15,18] but it does not correspond to a local minimum on the triplet PES as suggested in refs 15 and 18. Although a CP exists for an η^2-sulfoxide structure (*SO*-CP in Figure 2), this CP does not correspond to a minimum energy crossing point (MECP) in the multidimensional hypersurface of degeneracy (crossing seam).[20] In fact, MECPs were all found near the MC minima, and there is an extended low-lying triplet/singlet crossing seam that can be found in the MC PES region where efficient nonradiative decay could take place (see shaded area in Figure 2). *S*-$MECP_1$ (Figure S7, SI) and *S*-$MECP_2$ (Figure S8, SI) were located less than 1 and 4 kJ/mol above the *S*-MC_1 and *S*-MC_2 minima, respectively, while *O*-$MECP_1$ (Figure S9, SI) was found 10 kJ/mol above *O*-MC_1. Thus, the barriers to reach the *S*-$MECP_1$, *S*-$MECP_2$, and *O*-$MECP_1$ funnels are substantially lower than the adiabatic barriers required to overcome the *S*-MC-TS, *SO*-MC-TS, *O*-MC-MLCT-TS transition states, respectively, so that these funnels will be more easily accessible than the transition states. In the case of decay at *S*-$MECP_1$ or *S*-$MECP_2$, the adiabatic part of the isomerization required is the

dx.doi.org/10.1021/ja201625b | *J. Am. Chem. Soc.* 2011, 133, 9172–9174

partial de-coordination of the Ru−S bond to populate the *S*-linked MC minima. From these MECPs, the system can return to the *S*-bonded ground state or form the *O*-bonded ground state photoproduct. It is highly probable that the phase of the Ru−S and Ru−O_1 stretching modes at the time of decay will play a crucial role in the back formation of reactant versus formation of photoproduct. If the system decays at *SO*-CP or *O*-$MECP_1$, the photoisomerization involves a further adiabatic step, which is the rotation of the sulfoxide group (fourth adiabatic step). To have a complete adiabatic photoisomerization, formation of the new Ru−O_1 bond needs to occur in the triplet state. However, the activation barrier in the fifth adiabatic step is much larger than the one to access the *O*-$MECP_1$ funnel. Thus, nonradiative decay back to the ground state is more likely, and the Ru−O_1 bond formation will occur in this state.

From these results, we can conclude that nonadiabatic photoisomerization is expected to be more efficient than adiabatic photoisomerization in the case of $[Ru(bpy)_2(OSO)]^+$. In particular, formation of *O*-$MLCT_1$, which in addition requires overcoming the largest activation barrier, will be efficiently prevented by the presence of easily accessible funnels, in agreement with the experimental observations. However, the calculations also demonstrate that the photoisomerization will involve an excursion on the triplet PES in the region of ^{3}MC states, which was not inferred from the reported experimental observations. Future work will aim at understanding the photoisomerization mechanism of osmium sulfoxide complexes,[21] since the ^{3}MC states are inaccessible in such heavy-metal complexes. Also, one needs to revisit the photoisomerization mechanism of monodentate sulfoxide ruthenium complexes such as $[Ru(bpy)(tpy)(dmso)]^{2+}$ with a similar theoretical approach, in order to explain why an adiabatic mechanism is preferred in these systems.

■ ASSOCIATED CONTENT

Supporting Information. Computational details. Tables S1−S11 for optimized Cartesian coordinates, electronic structures and energies of all the stationary points. Figures S1−S5 for results of intrinsic reaction coordinate calculations. Figure S6 for complete potential energy profile. Figures S7−S9 for characterization of MECPs. Description of the animations. Complementary references. Animations of the photoisomerization steps. This material is available free of charge via the Internet at http://pubs.acs.org.

■ AUTHOR INFORMATION

Corresponding Author
martial.boggio@irsamc.ups-tlse.fr

■ ACKNOWLEDGMENT

This work was performed using HPC resources from CALMIP (Grant 2010-p0880).

■ REFERENCES

(1) Rack, J. J.; Winkler, J. R.; Gray, H. B. *J. Am. Chem. Soc.* **2001**, *123*, 2432–2433.
(2) Rack, J. J.; Mockus, N. V. *Inorg. Chem.* **2003**, *42*, 5792–5794.
(3) Rack, J. J.; Rachford, A. A.; Shelker, A. M. *Inorg. Chem.* **2003**, *42*, 7357–7359.
(4) Rachford, A. A.; Petersen, J. L.; Rack, J. J. *Inorg. Chem.* **2005**, *44*, 8065–8075.
(5) Rachford, A. A.; Petersen, J. L.; Rack, J. J. *Inorg. Chem.* **2006**, *45*, 5953–5960.
(6) Butcher, D. P.; Rachford, A. A.; Petersen, J. L.; Rack, J. J. *Inorg. Chem.* **2006**, *45*, 9178–9180.
(7) Rachford, A. A.; Rack, J. J. *J. Am. Chem. Soc.* **2006**, *128*, 14318–14324.
(8) Rachford, A. A.; Petersen, J. L.; Rack, J. J. *J. Chem. Soc., Dalton Trans.* **2007**, 3245–3251.
(9) Mockus, N. V.; Marquard, S.; Rack, J. J. *J. Photochem. Photobiol. A: Chem.* **2008**, *200*, 39–43.
(10) Mockus, N. V.; Rabinovich, D.; Petersen, J. L.; Rack, J. J. *Angew. Chem., Int. Ed.* **2008**, *47*, 1458–1461.
(11) Lutterman, D. A.; Rachford, A. A.; Rack, J. J.; Turro, C. *J. Phys. Chem. A* **2009**, *113*, 11002–11006.
(12) McClure, B. A.; Rack, J. J. *Angew. Chem., Int. Ed.* **2009**, *48*, 8556–8558.
(13) Dieckmann, V.; Eicke, S.; Rack, J. J.; Woike, T.; Imlau, M. *Opt. Exp.* **2009**, *17*, 15052–15060.
(14) Rack, J. J. *Coord. Chem. Rev.* **2009**, *253*, 78–85.
(15) McClure, B. A.; Mockus, N. V.; Butcher, D. P.; Lutterman, D. A.; Turro, C.; Petersen, J. L.; Rack, J. J. *Inorg. Chem.* **2009**, *48*, 8084–8091.
(16) McClure, B. A.; Abrams, E. R.; Rack, J. J. *J. Am. Chem. Soc.* **2010**, *132*, 5428–5436.
(17) Grusenmeyer, T. A.; McClure, B. A.; Ziegler, C. J.; Rack, J. J. *Inorg. Chem.* **2010**, *49*, 4466–4470.
(18) McClure, B. A.; Rack, J. J. *Eur. J. Inorg. Chem.* **2010**, 3895–3904.
(19) Ciofini, I.; Daul, C. A.; Adamo, C. *J. Phys. Chem. A* **2003**, *107*, 11182–11190.
(20) (a) Yarkony, D. R. *Rev. Mod. Phys.* **1996**, *68*, 985–1013. (b) Levine, B. G.; Martínez, T. J. *Annu. Rev. Phys. Chem.* **2007**, *58*, 613–634.(c) Bearpark, M. J.; Robb, M. A. In *Reviews of Reactive Intermediate Chemistry*; Platz, M. S., Moss, R. A., Jones Jr., M., Eds.; John Wiley & Sons, Inc.: NJ, 2007; pp 379−414 and references therein.
(21) Mockus, N. V.; Petersen, J. L.; Rack, J. J. *Inorg. Chem.* **2006**, *45*, 8–10.